Strongly Convergent Green's Function Expansions for Rectangularly Shielded Microstrip Lines

JOHN G. FIKIORIS, JOHN L. TSALAMENGAS, MEMBER, IEEE, AND GEORGE J. FIKIORIS

Abstract —The exact analytical treatment of the quasi-TEM mode in various cross-sectional configurations of microstrip lines may be based on Carleman-type singular integral equations (SIE's). Their kernel is a Laplacian Green's function G with source point limited on the interface separating the dielectric media. Strongly convergent expansions for G, particularly suited for the subsequent solution of the SIE and for exact field-point evaluations in rectangularly shielded microstrip configurations, are developed. Extraction of the singular logarithmic term leads to rapidly converging series expansions for the nonsingular part. The convergence of certain of these series is further improved when the field point lies also on the interface or when the source point approaches the shielding boundaries. In the first case, occurring typically in the kernel of integral equations, the Watson transformation provides alternative and exponentially convergent expansions for series converging slowly in the original G expression; in the second case, image source terms are further extracted out of G, leading to improved expansions for its remaining part. Numerical evaluations and comparisons illuminating these points are included.

I. Introduction

In a series of recent papers by the authors [1]–[3] an exact analytical approach was developed for the treatment of problems involving boundaries of different shapes. The method was applied to shielded lines with round conductors [3] and, in an accompanying paper [4], to rectangularly shielded striplines and printed microstrip lines. Crucial to this approach is the availability of strongly and uniformly convergent eigenfunction expansions for the Green's function G of the configuration, which appears as the kernel of the SIE and, subsequently, in the integrals that serve to evaluate the field of any point inside the guide. The SIE is of the Hilbert type for round conductors [3] and of the Carleman type for strip ones [4]. Its solution follows the Carleman–Vekua method, otherwise known as the method of regularization by solving the dominant equation [3], [4].

This paper is devoted to the development of various analytic and strongly convergent expressions for the Laplacian Green's function $G(x, y; x', 0)$ appropriate to a rectangularly shielded microstrip line (shown in Fig. 1) with two dielectric sublayers ϵ_1, ϵ_2 divided by the surface $y = 0$, on which the source point of G lies ($y' = 0$). The special case $\epsilon_1 = \epsilon_2$ was fully treated in [2] and finds application in the exact treatment of the TEM mode in rectangularly shielded lines with round conductors [3] or with strip conductors (striplines) [4]. As explained in [2], existing developments for this G are useless for exact solutions of SIE and related field-point evaluations, owing to their lack of convergence and uniformity of expression when the field point approaches or moves past the source point. The new expansions given in [2] have the singular logarithmic term extracted out of G in closed form, along with certain other simple harmonic terms, in a way that helps to improve the convergence of the expansion of the remaining, nonsingular part of G. The strong (exponential) convergence of the resulting expression of G can be further improved in particular situations ($y = y' = 0$, source point near the shielding walls) by special analytical techniques (Watson transformation, extraction of image source terms) and the improvement is, moreover, reflected in the stability and quick convergence of the TEM field expressions that result from the solution of the SIE [3], [4]. These two features, namely, exact and quickly obtained solutions, even in cases of close proximity of the conductors to the walls, and exact field evaluations at any point inside the guide, are, in the authors' opinion, unique to this analytical approach. Numerical methods (Galerkin, finite differences, etc.) are adequate for quantities such as the characteristic impedance, owing to the variational character of the basic integral formula. Their accuracy is very much reduced in

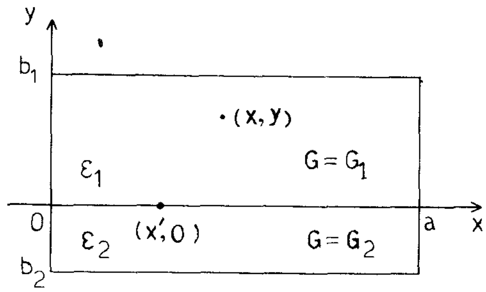

Fig. 1 The shielded line configuration with the line source on the dielectric interface.

Manuscript received March 28, 1987; revised November 28, 1987, and May 10, 1988.

The authors are with the Department of Electrical Engineering, National Technical University of Athens, Greece.

IEEE Log Number 8822908.

0018-9480/88/1000-1386$01.00

the case of close proximity or when the $\boldsymbol{E}$ and $\boldsymbol{H}$ fields are evaluated at any point inside the guide, particularly near sources and walls [5]–[8]. The G functions used in certain of these approaches [8]–[10] converge slowly (actually conditionally) and are inadequate in the aforementioned situations.

In the case of printed microstrip lines, $\epsilon_1 \neq \epsilon_2$, no pure TEM mode can propagate [5]–[9]. However, when the guide dimensions are much smaller than the wavelength $(a, b_1 - b_2 \ll \lambda)$ the E_z, H_z components of the principal hybrid mode are negligible compared with the transverse ones, and the latter can be well approximated by those of the so-called quasi-TEM mode; these then follow from Laplace's, rather than Helmholtz's, equation. The analytical treatment of this case leads again to a Carleman-type integral equation for the surface charge distribution $\sigma(x)$ (C/m^2) on the strip having as kernel the Green's function of the structure shown in Fig. 1; this function satisfies the following boundary value problem (BVP):

$$G(x,y;x',0) \equiv G_1(x,y;x') \qquad \text{in } 0 \leqq y \leqq b_1$$

$$G(x,y;x',0) \equiv G_2(x,y;x') \qquad \text{in } b_2 \leqq y \leqq 0 \qquad (1)$$

$$\left(\frac{\partial^2}{\partial x^2}+\frac{\partial^2}{\partial y^2}\right)G(x,y;x',0) = -2\pi\delta(x-x')\delta(y),$$
$$0 \leqq x, x' \leqq a;\ b_2 \leqq y \leqq b_1 \qquad (2)$$

$$G_1(0,y;x') = G_2(0,y;x') = G_1(a,y;x') = G_2(a,y;x') = G_2(x,b_2;x') = G_1(x,b_1;x') = 0 \qquad (3)$$

$$G_1(x,0^+;x') = G_2(x,0^-;x') \qquad 0 \leqq x, x' \leqq a \qquad (4)$$

$$\epsilon_1 \frac{\partial G_1}{\partial y}\bigg]_{y=0^+} = \epsilon_2 \frac{\partial G_2}{\partial y}\bigg]_{y=0^-} \qquad 0 \leqq x, x' \leqq a. \qquad (5)$$

With this definition of G the electrostatic potential of a line charge q (C/m) at $(x',0)$ is $\psi(x,y) = qG/\pi(\epsilon_1+\epsilon_2)$. Also, in the absence of any shielding walls,

$$G = G^p(x,y;x') = -\frac{1}{2}\ln\left[(x-x')^2+y^2\right];\ \psi(x,y) = -\frac{q\ln\left[(x-x')^2+y^2\right]}{2\pi(\epsilon_1+\epsilon_2)}. \qquad (6)$$

The solution of BVP (1)–(5) will be obtained in three forms, depending on the relative position of the field and source points, their proximity to the shielding walls, and whether the field point is near the separating surface $y = 0$. Thus, as in [2], in the next section we initially extract out of G the singular logarithmic term G^p defined in (6) and certain additional simple harmonic terms that help improve the uniform convergence of the remaining nonsingular part of G. The latter is expanded into appropriate harmonic series $S_j^{(1)}$ and $S_j^{(2)}$ $(j = 1,2,3,4)$ pertaining to regions 1 $(0 \leqq y \leqq b_1)$ and 2 $(b_2 \leqq y \leqq 0)$, respectively, and connected to each other through the boundary conditions (3)–(5). These series exhibit an exponential rate of convergence everywhere except in two special situations. The first is when both the field and the source point are located very near the shielding walls. In this case the influence of the nearby image source terms becomes predominant and destroys the convergence of the series $S_j^{(1)}, S_j^{(2)}$ [2], [3]. Extraction of corresponding logarithmic terms restores the convergence of the remaining series expansions in the second form of G thus obtained. This evaluation is carried out in Section III. It is very useful whenever the strip conductor approaches any of the four walls. The second situation is when $y = 0$. Here, the field point lies, also, on the dielectric interface, a situation that comes up in the formulation of a SIE for the shielded microstrip. As will be seen—and has already been observed in other situations [1]—the series $S_2^{(k)}$ $(k = 1,2)$ in the first form of G (and the corresponding ones in its second form) lose their exponential rate of convergence, exhibiting a slow uniform convergence of the order $1/m^2$, where m is the summation index. This slows down considerably the evaluation of G at such points and the solution of the SIE for microstrips. Application of Watson's transformation on $S_2^{(k)}$ in a way similar to [1] yields equivalent series that converge exponentially even when $y = 0$. This third form of G, developed in Section IV, improves drastically the solution of the microstrip SIE [4]. The numerical results of Section V illustrate the characteristics of the various forms of G outlined above.

II. The Original G Function

As outlined in the previous section and by analogy with [2] we can write down for G the following expressions:

$$G_k(x,y;x') = G^p(x,y;x') + G_k^c(x,y;x'), \qquad k = 1,2 \qquad (7)$$

which describe the solution of the inhomogeneous equation (2) in regions 1 and 2 in terms of its partial and complementary solutions G^p and G_k^c. The first, given in (6), follows from the well-known electrostatic solution of a line source q at the point x', y' in a medium ϵ_1 in $y \geqq 0$ separated from a medium ϵ_2 in $y \leqq 0$ in the limit $y' = 0$; at this limit G^p gets the unified form (6) valid in both $y \geqq 0$ and $y \leqq 0$ and accounts fully for the singular behavior of G near the source point. The complementary solution G_k^c is nonsingular throughout the region $0 \leqq x \leqq a$, $b_2 \leqq y \leqq b_1$ and, as in [2], after extracting out of it certain simple harmonic terms, may be expanded in four sine–sinh Fourier series $S_j^{(k)}(x,y)$ $(j = 1,2,3,4)$ in each region $k = 1$

and $k=2$:

$$G_k^c(x; y, x') = \frac{1}{ab_k}\Big\{(a-x)(b_k-y)\ln x' + x(b_k-y)\ln(a-x') + \frac{1}{2}(a-x)y\ln(x'^2+b_k^2) + \frac{1}{2}xy\ln\left[(a-x')^2+b_k^2\right]\Big\} + \sum_{j=1}^{4} S_j^{(k)}(x,y), \qquad k=1,2 \tag{8}$$

$$S_1^{(k)}(x,y) = \sum_{m=1}^{\infty} \alpha_{1m}^{(k)} \sin\frac{m\pi x}{a} \sinh\frac{m\pi y}{a} \tag{9a}$$

$$S_2^{(k)}(x,y) = \sum_{m=1}^{\infty} \alpha_{2m}^{(k)} \sin\frac{m\pi x}{a} \sinh\left[\frac{m\pi}{a}(b_k-y)\right] \tag{9b}$$

$$S_3^{(k)}(x,y) = \sum_{m=1}^{\infty} \alpha_{3m}^{(k)} \sin\frac{m\pi y}{b_k} \sinh\frac{m\pi x}{b_k} \tag{9c}$$

$$S_4^{(k)}(x,y) = \sum_{m=1}^{\infty} \alpha_{4m}^{(k)} \sin\frac{m\pi y}{b_k} \sinh\left[\frac{m\pi}{b_k}(a-x)\right]. \tag{9d}$$

The role of the extracted simple harmonic terms in (8) may be appreciated when the boundary conditions (3)–(5) are applied. For instance the third and fourth of the conditions in (3), $G_k(a, y; x') = 0$ $(k=1,2)$, lead to the relations

$$S_3^{(k)}(a,y) = \sum_{m=1}^{\infty} \alpha_{3m}^{(k)} \sinh\frac{m\pi a}{b_k} \sin\frac{m\pi y}{b_k} = \frac{1}{2}\ln\left[(a-x')^2+y^2\right] - \frac{b_k-y}{b_k}\ln(a-x') - \frac{y}{2b_k}\ln\left[(a-x')^2+b_k^2\right], \qquad y \text{ in } [0, b_k]. \tag{10}$$

The series on the left represents the Fourier-sine expansion of the simple function of y on the right, which vanishes at the end points $y=0$ and $y=b_k$ of the interval. This fact improves the convergence of the series $S_3^{(k)}(a,y)$ and, as is soon to be seen, makes the convergence of $S_3^{(k)}(x,y)$ uniform, of the order at least $1/m^3$, ensuring a convergence for the derivatives of G_k (i.e., of the field) of order at least $1/m^2$. Analogous conclusions can be drawn for the series $S_1^{(k)}(x,y)$, $S_4^{(k)}(x,y)$. The simple harmonic terms act as smoothing functions improving the convergence of the individual series, a property discussed further in [1]–[3]. In addition, they do not complicate the application of condition (4) at $y=0$, as will be verified below.

The expansion coefficients $\alpha_{3m}^{(k)}$ follow from (10) and the orthogonality of $\{\sin(m\pi y/b_k)\}$ in $[0, b_k]$. The integrations of the right-hand side are the same as those carried out in [2] and yield

$$\alpha_{3m}^{(k)} = -d_m\left[\frac{\pi}{b_k}(-a+x')\right]\Big/\left(m\pi\sinh\frac{m\pi a}{b_k}\right) \tag{11}$$

$$\begin{aligned} d_m(z) &= \mathrm{Re}\{\exp(mz)[E_1(mz-im\pi)-E_1(mz)] + \exp(-m\bar{z})[E_1(-m\bar{z}-im\pi)-E_1(-m\bar{z})]\} \\ &= d_m(-\bar{z}) \\ &\underset{m\to\infty}{\sim} \frac{2}{m^2}\mathrm{Re}\left[z^2/|z|^4-(-1)^m(z-i\pi)^2 /|z-i\pi|^4\right] + O(1/m^3) \end{aligned} \tag{12}$$

$E_1(z)$ being the exponential integral function [11], whose numerical evaluation and asymptotic behavior are discussed in [1]–[3] and [11]. Also, $\bar{z}$ is the complex conjugate of z.

In a similar way the remaining boundary conditions in (3): $G_k(0, y; x') = G_k(x, b_k; x') = 0$ provide relations from which the coefficients $\alpha_{1m}^{(k)}, \alpha_{4m}^{(k)}$ are obtained as follows:

$$\alpha_{1m}^{(k)} = -\frac{1}{m\pi\sinh\frac{m\pi b_k}{a}}\left\{2\pi\sin\left(\frac{m\pi x'}{a}\right)\exp\left(-\frac{m\pi|b_k|}{a}\right) + d_m\left[\frac{\pi}{a}(-b_k+jx')\right]\right\} \tag{13}$$

$$\alpha_{4m}^{(k)} = -d_m\left(-\frac{\pi}{b_k}x'\right)\Big/\left(m\pi\sinh\frac{m\pi a}{b_k}\right). \tag{14}$$

The results of (11)–(14), which are identical to those in [2] with $y'=0$, determine completely the series S_1, S_3, S_4. Their convergence follows from the behavior of their general terms as $m\to\infty$ and is the same as in the corresponding series of [2] with $y'=0$ (see also [3] and (12)). The final results are

$$\left|\alpha_{1m}^{(k)}\sin\frac{m\pi x}{a}\sinh\frac{m\pi y}{a}\right| < \frac{2}{m}\exp\left[-\frac{m\pi}{a}(2|b_k|-|y|)\right] + \frac{2a^2}{\pi^3 m^3}\exp\left[-\frac{m\pi}{a}(|b_k|-|y|)\right] \cdot\left|\frac{b_k^2-x'^2}{(b_k^2+x^2)^2}-(-1)^m\frac{b_k^2-(a-x')^2}{\left[b_k^2+(a-x')^2\right]^2}+O(1/m)\right| \tag{15a}$$

$$\left|\alpha_{3m}^{(k)}\sin\frac{m\pi y}{b_k}\sinh\frac{m\pi x}{b_k}\right| < \frac{2b_k^2}{\pi^3 m^3}\exp\left[-\frac{m\pi}{|b_k|}(a-x)\right]\cdot\left|\frac{1}{(a-x')^2}-(-1)^m\frac{(a-x')^2-b_k^2}{\left[(a-x')^2+b_k^2\right]^2}+0(1/m)\right| \tag{15b}$$

$$\left|\alpha_{4m}^{(k)}\sin\frac{m\pi y}{b_k}\sinh\left[\frac{m\pi}{b_k}(a-x)\right]\right| < \frac{2b_k^2}{\pi^3 m^3}\exp\left(-\frac{m\pi x}{|b_k|}\right)\cdot\left|\frac{1}{x'^2}-(-1)^m\frac{x'^2-b_k^2}{(x'^2+b_k^2)^2}+0(1/m)\right|. \tag{15c}$$

The exponential rate of convergence is made obvious by these relations and is further strengthened by the factors $1/m$ and $1/m^3$. This rate is lost for the series $S_3^{(k)}$ (or $S_4^{(k)}$) when $x \cong a$ (or $x \cong 0$) and for the series $S_1^{(k)}$ when $|y| = |b_k|$, but the convergence remains uniform, of the order $1/m^3$. Only when both x and x' approach a (or 0), i.e., when both the field and source points approach very near the shielding wall $x = a$ (or $x = 0$), the series $S_3^{(k)}$ (or $S_4^{(k)}$) fail to converge. This, as already mentioned, is due to the strong influence of the nearby image source and can be remedied by extracting out of G_k further logarithmic terms, a procedure carried out in Section III below.

It remains to determine the coefficients $\alpha_{2m}^{(k)}$ ($k = 1,2$) by applying the last boundary conditions (4) and (5). Substituting (6)–(9) in (4) leads directly to

$$\alpha_{2m}^{(1)} \sinh \frac{m\pi b_1}{a} = \alpha_{2m}^{(2)} \sinh \frac{m\pi b_2}{a} \tag{16}$$

while invoking (5), the fact that $[\partial G^p/\partial y]_{y=0} = 0$ and the orthogonality of $\{\sin(m\pi x/a)\}$ ($m = 1,2,\cdots$), we end up with the relations

$$\begin{aligned}\alpha_{2m}^{(1)} \sinh \frac{m\pi b_1}{a} &= \alpha_{2m}^{(2)} \sinh \frac{m\pi b_2}{a} \\ &= \frac{1}{B_m}\Bigg\{\frac{2}{a}\left(\frac{a}{m\pi}\right)^2\left[(-1)^{m+1}g(a-x') + g(x')\right] \\ &\quad - \sum_{l=1,2}(-1)^l \epsilon_l \alpha_{1m}^{(l)} \\ &\quad + \frac{2}{a}\sum_{l=1,2}(-1)^{l+1}\sum_{q=1}^{\infty}\frac{\epsilon_l}{b_l}\left\{(-1)^m d_q\left[\frac{\pi}{b_l}(-a+x')\right]\right. \\ &\quad \left. - d_q\left(-\frac{\pi x'}{b_l}\right)\right\}\frac{1}{\left(\frac{m\pi}{a}\right)^2 + \left(\frac{q\pi}{b_l}\right)^2}\Bigg\}\end{aligned} \tag{17}$$

$$B_m = \epsilon_1 \coth \frac{m\pi b_1}{a} - \epsilon_2 \coth \frac{m\pi b_2}{a} \tag{18}$$

$$g(x) = \frac{\epsilon_1}{2b_1}\ln(x^2 + b_1^2) - \frac{\epsilon_2}{2b_2}\ln(x^2 + b_2^2) - \left(\frac{\epsilon_1}{b_1} - \frac{\epsilon_2}{b_2}\right)\ln|x| \tag{19}$$

where $\alpha_{1m}^{(l)}$ are given in (13).

Inspection of (17) reveals that the series S_2 defined in (9b) exhibits an exponential convergence when the observation point is not near the dielectric interface. However, when $y \to 0$, as pointed out previously, the general term of S_2 loses its exponential decay, behaving asymptotically only as $(-1)^m/m^2$. This defect will be remedied in Section IV by applying the transformation of Watson.

In this section we have derived in effect a unified expression for the G function of the structure in separated form, characterized by a very rapid rate of convergence everywhere except in the cases noted above.

III. The Second Form of the G Function

As discussed previously in connection with (15b), (15c) the series S_3, S_4 fail to converge when $x' \cong a$ or $x' \cong 0$, respectively. This is attributed to the influence of the nearby image logarithmic source when the observation point $(x',0)$ approaches the shielding walls, whose nearly singular behavior destroys the convergence of the series. This argument suggests, also, the way to remedy the situation by extracting out of G_k^c further logarithmic terms, corresponding to line sources at $(2a - x',0)$ and $(-x',0)$:

$$\begin{aligned}G_k^c(x,y;x') &= \frac{1}{2}\ln\left[(x+x'-2a)^2 + y^2\right] \\ &\quad + \frac{1}{2}\ln\left[(x+x')^2 + y^2\right] \\ &\quad - \frac{1}{ab_k}\Bigg\{(a-x)(b_k-y) \\ &\quad \cdot\ln(2a-x') + x(b_k-y)\ln(a+x') \\ &\quad + \frac{1}{2}(a-x)y\ln\left[(2a-x')^2 + b_k^2\right] \\ &\quad + \frac{xy}{2}\ln\left[(a+x')^2 + b_k^2\right]\Bigg\} \\ &\quad + \sum_{j=1}^{4} S_j'^{(k)}(x,y), \qquad k = 1,2.\end{aligned} \tag{20}$$

The series $S_j'^{(k)}(x,y)$ ($j = 1,2,3,4$) are the same as $S_j^{(k)}(x,y)$ in (9) with new coefficients $\alpha_{jm}'^{(k)}$ in place of $\alpha_{jm}^{(k)}$.

Applying the boundary conditions at $x = a$, $x = 0$, $y = b_k$ as before, we obtain first expressions for the coefficients $\alpha_{jm}'^{(k)}$ for $j = 1,3,4$:

$$\begin{aligned}\alpha_{1m}'^{(k)} &= \frac{1}{m\pi\sinh\left(\frac{m\pi}{a}b_k\right)}\Bigg\{-2\pi\sin\left(\frac{m\pi}{a}x'\right) \\ &\quad \cdot\exp\left(-\frac{m\pi}{a}|b_k|\right) - d_m\left[\frac{\pi}{a}(-b_k + ix')\right] \\ &\quad + d_m\left[\frac{\pi}{a}(-b_k - ix')\right] \\ &\quad + d_m\left[-\frac{\pi}{a}b_k - i\frac{\pi}{a}(x'-2a)\right]\Bigg\}\end{aligned} \tag{21}$$

$$\alpha_{3m}'^{(k)} = \frac{1}{m\pi\sinh\frac{m\pi a}{b_k}}d_m\left[\frac{\pi}{b_k}(-a'-x')\right];$$

$$\alpha_{4m}'^{(k)} = \frac{1}{m\pi\sinh\frac{m\pi a}{b_k}}d_m\left[\frac{\pi}{b_k}(x'-2a)\right]. \tag{22}$$

For large m use of (12) shows that the general term of $S_j'^{(k)}$ $(j=1,3,4)$ behaves as follows:

$$\left|\alpha_{1m}'^{(k)}\sin\left(\frac{m\pi x}{a}\right)\sinh\left(\frac{m\pi y}{a}\right)\right| < \frac{2}{m}\exp\left[-\frac{m\pi}{a}(2|b_k|-|y|)\right] + \frac{2a^2}{\pi^3 m^3}\exp\left[-\frac{m\pi}{a}(|b_k|-|y|)\right] \cdot\left|\frac{b_k^2-(x'-2a)^2}{\left[b_k^2+(x'-2a)^2\right]^2}-(-1)^m \cdot\frac{b_k^2-(x'+a)^2}{\left[b_k^2+(x'+a)^2\right]^2}+0(1/m)\right| \tag{23a}$$

$$\left|\alpha_{3m}'^{(k)}\sin\left(\frac{m\pi y}{b_k}\right)\sinh\left(\frac{m\pi x}{b_k}\right)\right| < \frac{2b_k^2}{\pi^3 m^3}\exp\left[-\frac{m\pi}{|b_k|}(a-x)\right] \cdot\left|\frac{1}{(a+x')^2}-(-1)^m\frac{(a+x')^2-b_k^2}{\left[(a+x')^2+b_k^2\right]^2}+0(1/m)\right| \tag{23b}$$

$$\left|\alpha_{4m}'^{(k)}\sin\left(\frac{m\pi y}{b_k}\right)\sinh\left[\frac{m\pi}{b_k}(a-x)\right]\right| < \frac{2b_k^2}{\pi^3 m^3}\exp\left(-\frac{m\pi x}{|b_k|}\right)\cdot\left|\frac{1}{(x'-2a)^2}-(-1)^m \cdot\frac{(x'-2a)^2-b_k^2}{\left[(x'-2a)^2+b_k^2\right]^2}+0(1/m)\right|. \tag{23c}$$

Now, obviously, as x' approaches either a or 0, the series S_3', S_4' continue to converge exponentially, in contrast to the preceding expansions S_3, S_4, given in (9) and (15). When the observation point approaches the shielding walls ($|y|=|b_k|$ for $S_1'^{(k)}$, $x=a$ for S_3', and $x=0$ for S_4') the exponential decay is lost, but the series converge uniformly, at least as $1/m^3$. In any case when (x,y) approaches the shielding walls the result is known, $G\cong 0$, while when it moves very near $(x',0)$ the dominant logarithmic terms of the expansions account for the rapid change (singular behavior) of G; the remaining terms (simple harmonic and series) represent small correction and analytic terms which account for the influence on G of the dielectric interface and the charge distribution on the walls. When both x and x' are near a (or 0) and y is near 0, the two logarithmic terms (source and its nearby image) of the second expansion account for the dominant behavior of G, leaving the strong convergence of the series S_3' or S_4' undisturbed. Let us add at this point that the technique of extracting out of G the image source has been applied to scattering problems as well [12], [13].

Finally, application of the boundary conditions (4), (5) at $y=0$ provide, as previously, the coefficients $\alpha_{2m}'^{(k)}$ $(k=1,2)$:

$$\alpha_{2m}'^{(1)}\sinh\left(\frac{m\pi}{a}b_1\right) = \alpha_{2m}'^{(2)}\sinh\left(\frac{m\pi}{a}b_2\right) = \frac{1}{B_m}\left\{\frac{2}{a}\left(\frac{a}{m\pi}\right)^2\left[(-1)^m g(a+x')-g(2a-x')\right] - \sum_{l=1,2}(-1)^l\epsilon_l\alpha_{1m}'^{(l)} + \frac{2}{a}\sum_{l=1,2}(-1)^l\frac{\epsilon_l}{b_l}\sum_{q=1}^{\infty}\left\{(-1)^m d_q\left[\frac{\pi}{b_l}(-a-x')\right] - d_q\left[\frac{\pi}{b_l}(x'-2a)\right]\right\} \cdot\frac{1}{\left(\frac{m\pi}{a}\right)^2+\left(\frac{q\pi}{b_l}\right)^2}\right\}. \tag{24}$$

It is concluded from (24) that the general term of $S_2'^{(k)}(x,y)$ decays exponentially as $m\to\infty$ as long as the observation point is not located near the dielectric interface. However, when $y=0$ the rate of convergence of this series is of the order $(-1)^m/m^2$. The same behavior was noticed previously for the series $S_2^{(k)}(x,y)$ defined by (9b) and (17). By applying the method of Watson in the next section a drastic improvement is achieved for both these series.

IV. Application of Watson's Method: The Third G Expression

A detailed examination of the expressions (9b) and (17) for $S_2^{(k)}$ and (24) for $S_2'^{(k)}$ reveals that the loss of the exponential rate of convergence of these series as $y\to 0$ is due to terms of the form

$$\frac{2}{a}\frac{\sinh\left[\frac{m\pi}{a}(b_k-y)\right]}{B_m\sinh\left(\frac{m\pi}{a}b_k\right)}\left\{\begin{array}{c}\dfrac{(\pm 1)^m}{\left(\frac{m\pi}{a}\right)^2}\\[2ex] \dfrac{(\pm 1)^m}{\left(\frac{m\pi}{a}\right)^2+\left(\frac{q\pi}{b_l}\right)^2}\end{array}\right\}\cdot h(x'), \qquad (l=1,2)$$

appearing on the right-hand side of (17) and (24), respectively, while the remaining terms of (17) and (24) decay

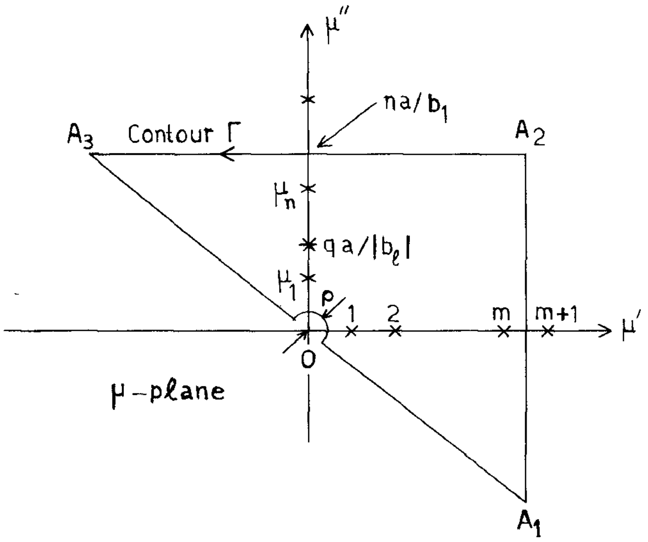

Fig. 2. Triangular contour Γ for the application of Watson's method.

exponentially with increasing m. So we concentrate on series of the form

$$S_{kl}^{\mp}=\sum_{m=1}^{\infty}\frac{(\mp 1)^m \sin\left(\frac{m\pi x}{a}\right)\sinh\left[\frac{m\pi}{a}(b_k-y)\right]}{\left[\left(\frac{m\pi}{a}\right)^2+\left(\frac{q\pi}{b_l}\right)^2\right]B_m \sinh\left(\frac{m\pi b_k}{a}\right)},$$

$$k=1,2;\; l=1,2;\; q=0,1,2,\cdots \tag{25}$$

and seek ways to improve their convergence for small y. To this end we may invoke the well-known Watson method [1], [2]. As a first step in the application of this technique we form the following contour integrals:

$$\oint_\Gamma f_{kl}^{\{\mp\}}(\mu)\,d\mu=\oint_\Gamma \frac{\begin{Bmatrix}\sin\left(\frac{\mu\pi x}{a}\right)\\ \sin\left[\frac{\mu\pi}{a}(x-a)\right]\end{Bmatrix}\sinh\left[\frac{\mu\pi}{a}(b_k-y)\right]}{\left[\left(\frac{\mu\pi}{a}\right)^2+\left(\frac{q\pi}{b_l}\right)^2\right]\sin(\pi\mu)\left[\epsilon_1\coth\left(\frac{\mu\pi b_1}{a}\right)-\epsilon_2\coth\left(\frac{\mu\pi b_2}{a}\right)\right]\sinh\left(\frac{\mu\pi b_k}{a}\right)}\,d\mu \tag{26}$$

along the closed triangular contour Γ in the μ plane shown in Fig. 2. The corners A_1, A_3 are symmetrical to A_2 with respect to the real and imaginary axes, respectively, the side A_1A_2 cuts the real axis at $\mu'=m+1/2$, while A_2A_3 cuts the imaginary axis at $\mu''=na/b_1$ $(n=1,2,\cdots)$. When $q=0$ the integrand $f_{kl}^{\{\mp\}}(\mu)$ has a simple pole at $\mu=0$ and A_3A_1 bypasses this point around a small circumference of radius ρ. When $q=1,2,\cdots$ the pole inside Γ is located at $\mu=i\mu''=iqa/|b_l|$ and A_3A_1 passes straight over $\mu=0$.

Obviously $f_{kl}^{\{\mp\}}(\mu)$ is an odd function of μ, so the integral over A_3A_1 vanishes. It is further shown in the Appendix that for all μ on A_1A_2 and A_2A_3 the integrand $f_{kl}^{\{\mp\}}(\mu)$ vanishes as these sides recede, independently, to ∞, i.e., as $\mu'=m+1/2\to\infty$ and as $\mu''=na/b_1\to\infty$. This means that at these limits the sum of residues of all poles of the integrand, enclosed in Γ, is 0. The poles and their corresponding residues in Γ are as follows.

a) At $\mu=m$ $(m=1,2,\cdots)$ with a sum of residues

$$\sum_{m=1}^{\infty}\operatorname{Res} f_{kl}^{\{\mp\}}(\mu=m)=S_{kl}^{\mp}/\pi. \tag{27}$$

b) At $\mu=iqa/|b_l|$ $(q=1,2,\cdots)$ with residue

$$\operatorname{Res} f_{kl}^{\{\mp\}}(\mu=iqa/|b_l|)=\frac{ab_l\sin(\pi qy/b_l)\,\delta\left(\frac{b_k}{b_l}q\right)\begin{Bmatrix}-\sinh\left(\frac{q\pi x}{b_l}\right)\\ \sinh\left[\frac{q\pi}{b_l}(a-x)\right]\end{Bmatrix}}{2q\pi^2 b_k\sinh\left(\frac{\pi qa}{b_l}\right)\left[\frac{\epsilon_1}{b_1}\delta\left(\frac{b_1}{b_l}q\right)-\frac{\epsilon_2}{b_2}\delta\left(\frac{b_2}{b_l}q\right)\right]} \tag{28}$$

where $\delta(x)=1$ for $x=$ integer, $\delta(x)=0$ otherwise. The correct evaluation of these residues requires special care when $(b_k/b_l)q$ is an integer.

For $q=0$ the pole is located at $\mu=0$ with residue:

$$\operatorname{Res} f_{kl}^{\{\mp\}}(\mu=0)=\frac{\begin{Bmatrix}x\\ x-a\end{Bmatrix}(1-y/b_k)}{\pi\left(\frac{\epsilon_1}{b_1}-\frac{\epsilon_2}{b_2}\right)}. \tag{29}$$

c) At the roots of the transcendental equation

$$\left[\epsilon_1\coth\left(\frac{\mu\pi b_1}{a}\right)-\epsilon_2\coth\left(\frac{\mu\pi b_2}{a}\right)\right]\sinh\left(\frac{\mu\pi b_k}{a}\right)=0 \tag{30}$$

which fall on the positive imaginary axis $\mu=i\mu''$ $(\mu''>0)$, at points $\mu''=\mu_n$ (>0) $(n=1,2,\cdots)$. It is shown in the Appendix that all the zeros of (30) are purely imaginary. The corresponding residues are

$$\operatorname{Res} f_{kl}^{\{\mp\}}(\mu=i\mu_n)=\frac{\begin{bmatrix}\sinh\left(\frac{x}{b_1}u_n''\right)\\ \sinh\left(\frac{x-a}{b_1}u_n''\right)\end{bmatrix}\sin\left(\frac{b_k-y}{b_1}u_n''\right)}{\left[\left(\frac{q\pi}{b_l}\right)^2-\left(\frac{u_n''}{b_1}\right)^2\right]\frac{\pi}{a}H_n\sin\left(\frac{b_k}{b_1}u_n''\right)},$$

$$q=0,1,2,\cdots \tag{31}$$

$$H_n=\sinh\left(\frac{a}{b_1}u_n''\right)\left[\frac{\epsilon_1 b_1}{\sin^2 u_n''}-\frac{\epsilon_2 b_2}{\sin^2(u_n''b_2/b_1)}\right] \tag{32}$$

with $\mu_n = (a/\pi b_1)u_n''$, where the positive values u_n'' are determined in the Appendix. It follows that the initial series $S_{kl}^{\mp}$, divided by π, can be expressed as the negative sum of the residue (28) when $q = 1, 2 \ldots$ (or half of the residue (29) when $q = 0$) plus the infinite series of the residues (31). The whole new expressions for $S_2^{(k)}$ in (9b), (17) and $S_2'^{(k)}$ in (24), thus obtained, are given below:

$$S_2^{(k)}(x,y) = -\sum_{m=1}^{\infty} \frac{\sin\left(\frac{m\pi x}{a}\right)\sinh\left[\frac{m\pi}{a}(b_k - y)\right]}{B_m \sinh\left(\frac{m\pi}{a}b_k\right)} \sum_{l=1,2}(-1)^l \epsilon_l \alpha_{1m}^{(l)} + \frac{1-\frac{y}{b_k}}{a\left(\frac{\epsilon_1}{b_1}-\frac{\epsilon_2}{b_2}\right)}$$
$$\cdot\left[xg(a-x') - (x-a)g(x')\right] - 2b_1^2 \sum_{n=1}^{\infty} \sin\left[\frac{u_n''}{b_1}(b_k - y)\right]\left[\sinh\left(\frac{x}{b_1}u_n''\right)g(a-x')\right.$$
$$\left.+\sinh\left(\frac{a-x}{b_1}u_n''\right)g(x')\right] \Big/ \left[u_n''^2 H_n \sin\left(\frac{b_k}{b_1}u_n''\right)\right]$$
$$-\sum_{l=1,2}(-1)^l \epsilon_l \sum_{q=1}^{\infty}\left\{\frac{\sin\left(\frac{\pi q y}{b_l}\right)\delta\left(\frac{b_k}{b_l}q\right)\left[\sinh\left(\frac{\pi q x}{b_l}\right)d_q\left(\pi\frac{x'-a}{b_l}\right)+\sinh\left(\pi q\frac{a-x}{b_l}\right)d_q\left(-\frac{\pi x'}{b_l}\right)\right]}{q\pi b_k \sinh\left(\frac{\pi q a}{b_l}\right)\left[\frac{\epsilon_1}{b_1}\delta\left(\frac{b_1}{b_l}q\right)-\frac{\epsilon_2}{b_2}\delta\left(\frac{b_2}{b_l}q\right)\right]}\right.$$
$$\left.-\frac{2}{b_l}\sum_{n=1}^{\infty}\frac{\sin\left(\frac{b_k-y}{b_1}u_n''\right)\left[\sinh\left(\frac{x}{b_1}u_n''\right)d_q\left(\pi\frac{x'-a}{b_l}\right)+\sinh\left(\frac{a-x}{b_1}u_n''\right)d_q\left(-\frac{\pi x'}{b_l}\right)\right]}{\left[\left(\frac{q\pi}{b_l}\right)^2-\left(\frac{u_n''}{b_1}\right)^2\right]H_n\sin\left(\frac{b_k}{b_1}u_n''\right)}\right\} \tag{33}$$

where $\alpha_{1m}^{(l)}$ is given in (13).

$$S_2'^{(k)}(x,y) = -\sum_{m=1}^{\infty} \frac{\sin\left(\frac{m\pi x}{a}\right)\sinh\left[\frac{m\pi}{a}(b_k - y)\right]}{B_m \sinh\left(\frac{m\pi}{a}b_k\right)} \sum_{l=1,2}(-1)^l \epsilon_l \alpha_{1m}'^{(l)} - \frac{1-\frac{y}{b_k}}{a\left(\frac{\epsilon_1}{b_1}-\frac{\epsilon_2}{b_2}\right)}$$
$$\cdot\left[g(a+x')x - g(2a-x')(x-a)\right] + 2b_1^2 \sum_{m=1}^{\infty} \sin\left[\frac{u_n''}{b_1}(b_k - y)\right]\left[\sinh\left(\frac{x}{b_1}u_n''\right)g(a+x')\right.$$
$$\left.+\sinh\left(\frac{a-x}{b_1}u_n''\right)g(2a-x')\right] \Big/ \left[u_n''^2 H_n \sin\left(\frac{b_k}{b_1}u_n''\right)\right] + \sum_{l=1,2}(-1)^l \epsilon_l$$
$$\cdot\sum_{q=1}^{\infty}\left\{\frac{\sin\left(\frac{\pi q y}{b_l}\right)\delta\left(\frac{b_k}{b_l}q\right)\left[\sinh\left(\pi q\frac{a-x}{b_l}\right)d_q\left(\pi\frac{x'-2a}{b_l}\right)+\sinh\left(\frac{\pi q x}{b_l}\right)d_q\left(-\pi\frac{a+x'}{b_l}\right)\right]}{q\pi b_k \sinh\left(\frac{\pi q a}{b_l}\right)\left[\frac{\epsilon_1}{b_1}\delta\left(\frac{b_1}{b_l}q\right)-\frac{\epsilon_2}{b_2}\delta\left(\frac{b_2}{b_l}q\right)\right]}\right.$$
$$\left.-\frac{2}{b_l}\sum_{n=1}^{\infty}\frac{\sin\left(\frac{b_k-y}{b_1}u_n''\right)\left[\sinh\left(\frac{a-x}{b_1}u_n''\right)d_q\left(\pi\frac{x'-2a}{b_l}\right)+\sinh\left(\frac{x}{b_1}u_n''\right)d_q\left(-\pi\frac{a+x'}{b_l}\right)\right]}{\left[\left(\frac{q\pi}{b_l}\right)^2-\left(\frac{u_n''}{b_1}\right)^2\right]H_n\sin\left(\frac{b_k}{b_1}u_n''\right)}\right\}. \tag{34}$$

TABLE I

$x' = 18$; D = DOMINANT TERM $= -\frac{1}{2}[\ln(x - x')^2 + y^2]$

x	y	G_α	M	G_β	M	G_γ	M	G_δ	M	D	G_δ-D
17	2	1.632002	19	1.631971	19	1 632002	6	1.631971	6	-0.8047190	2.436690
17	4	1.100459	15	1.100428	7	1 100459	6	1 100428	6	-1 416607	2.517035
19	4	1.089718	12	1.089684	9	1.089718	6	1.089684	6	-1 416607	2.506291
19	2	1.622276	21	1.622240	17	1 622276	6	1 622240	7	-0 8047190	2.426959
19	-2	1.507906	23	1.507876	17	1 507906	9	1.507876	7	-0.8047190	2.312595
19	-4	0 8530757	21	0.8530532	15	0.8530757	15	0.8530532	11	-1 416607	2.269660
17	-4	0.8582291	17	0.8582104	15	0.8582291	15	0.8582104	13	-1.416607	2 274817
17	-2	1.514747	22	1.514723	21	1.514747	9	1.514723	8	-0 8047190	2.319442
17	0	2.34072	63	2 34069	63	2 340719	6	2 340691	8	0	2.340691
17.5	0	3.03001	62	3.02998	60	3.030012	8	3 029984	7	0.6931472	2.336837
17 8	0	3.94462	67	3.94459	68	3.944620	6	3.944591	7	1.609438	2 335153
17 95	0	5 33025	68	5.33021	68	5.330249	6	5.330219	8	2.995732	2.334487
17.99	0	6.93953	68	6.93950	69	6.939529	9	6.939500	7	4.605170	2.334330
18.01	0	6.93945	69	6.93942	69	6.939454	6	6.939424	7	4.605170	2.334254
18.05	0	5.32987	69	5.32984	69	5 329871	6	5.329841	7	2.995732	2.334109
18.2	0	3 94311	67	3.94308	67	3.943106	8	3.943076	7	1 609438	2 333638
18 5	0	3.02622	65	3 02619	62	3.026224	6	3.026192	8	0.6931472	2.333045
19	0	2.33311	60	2.33308	60	2.333110	6	2 333077	7	0	2.333077

TABLE II

$x' = 29.9$; D = DOMINANT TERMS $= -\frac{1}{2}\ln[(x - x')^2 + y^2] + \frac{1}{2}\ln[(x + x' - 2a)^2 + y^2]$

x	y	M	G_α	G_β	G_γ	C_δ	D
		1	0.4520517	1.282328	3.699040	1,280485	
		10	0.7427881	1 282234	1 799159	1.281124	1.282475
29 85	0 05	70	1.198505	1.281547	1 292053	1 281352	
		1	0.7758923	1 416502	4.028069	1.414696	
		10	1 001345	1.416429	2.063884	1.415284	1.416607
29 90	0 05	70	1 333782	1 415850	1.437069	1 415623	
		1	0.4065871	0.8046559	3.669789	0.8028990	
		10	0.5668899	0 8046034	1 637953	0.8034310	0.8047190
29 95	0.05	70	0.7663978	0 8041354	0 8514662	0 8039343	
		1	0.4304006	0.8046673	3.717696	0.8028606	
		10	0.6074180	0.8044452	1.682531	0.8032730	0.8047190
29 95	-0 05	70	0 7467897	0 8041322	0 8379124	0.8039319	
		1	0.7992161	1.416513	4.070663	1 414656	
		10	1.036353	1 416292	2.098527	1.415147	1.416607
29.90	-0 05	70	1.326294	1.415847	1.431185	1 415620	
		1	4748963	1.282339	3.739704	1.280444	
		10	7730518	1 282115	1.827993	1 281005	1 282475
29 85	-0 05	70	1 195549	1 281544	1.289528	1 281350	
		1	0 7622708	1 609313	4.180658	1 607185	
		10	0.9772221	1.609237	2 179648	1 607889	1.609438
29.85	0	70	1.470025	1 608638	1 619108	1 608335	
		1	1.664737	2.397796	5 090760	2.395661	
		10	1 836793	2 397735	3.048791	2.396337	? 39789
29.88	0	70	2 239570	2 397243	2.413090	2.396875	
		1	2.353276	3.044432	5.781838	3.042295	
		10	2 511018	3.044376	3 725934	3.042961	3.044522
29.89	0	70	2.882487	3.043922	3.062300	3 043535	
		1	2 344060	2.944365	5 777693	2 942224	
		10	2.473157	2.944319	3.693485	2.942870	2.944439
29.91	0	70	2.780324	2.943943	2 969010	2.943523	
		1	1 646304	2.197159	5.082469	2.195016	
		10	1.761070	2.197118	2.983888	2.195651	2.197225
29.92	0	70	2.035342	2.196782	2.226252	2 196348	
		1	0.7161889	1.098571	4 159932	1.096423	
		10	0 7879365	1.098546	2.017327	1.097026	1 098612
29 95	0	70	0 9611400	1.098333	1 147468	1.097877	
		1	0.370500	0.6190147	3.819282	0 6168625	
		10	0 4135532	0.6189996	1.646553	0.6174423	0.6190392
29.97	0	70	0.5179179	0.6188710	0 6894942	0.6184174	
		1	0.1099689	0 2006626	3.563779	0 1985066	
		10	0 1243207	0 2006575	1.360288	0.1990626	0 2006707
29.99	0	70	0 1591830	0 2006146	0 3041360	0.2001828	

In both $S_2^{(k)}$ and $S_2'^{(k)}$ the slowly converging series over m, when $|y|$ is small or 0, are substituted by exponentially converging series over n. Indeed, the dependence on y appears now in sine instead of sinh functions, while $\sinh(u_n''x/b_1)$ and $\sinh(u_n''(a-x)/b_1)$ in the numerator are divided by $\sinh(u_n''a/b_1)$, thus securing an exponential decay of the series. Even the convergence rate of the series over q is now improved. On the interface, for $y=0$, both (33) and (34) are simplified considerably.

V. Numerical Results and Conclusions

Four expressions for $G_k(x, y; x')$ $(k=1,2)$ have been obtained. The first, denoted from here on as G_α, is defined in (7)–(9), (11)–(14), and (17) and converges rapidly when the source point $(x',0)$ is not very near the shielding walls $x=0, a$. The second, G_β, defined in (7), (9), (20)–(22), and (24), takes into account the influence of the image sources in closed form and converges rapidly even when x' is near 0 or a. The third and fourth G_γ, G_δ, obtained via the transformation of Watson, provide alternative and rapidly converging series for the sums $S_2^{(k)}$ and $S_2'^{(k)}$ of G_α and G_β, respectively, when the field point (x, y) is near the interface $y=0$. The remaining parts of G_α, G_β remain the same in the expressions G_γ, G_δ. The equations defining these new expressions for $S_2^{(k)}$ and $S_2'^{(k)}$ are (33) and (34), respectively.

In the following tables values of G from all four expressions are given for various positions of the source and field points. The geometry of the shielded line is kept the same in all tables: $a=30$, $b_1=16$, $b_2=-8$, $\epsilon_1=1$, $\epsilon_2=10$. In Table I the source point is away from the walls, $x'=18$, while the field point moves around it. Apart from the four values of G we provide in each case the approximate number M of terms, used in the basic summations over m (over n for the sums $S_2^{(k)}, S_2'^{(k)}$ in G_γ, G_δ), at which the final value of G settles to the indicated accuracy, thus providing a clear criterion of the rate of convergence. We also provide the value of the dominant term D, in this case $D=-\frac{1}{2}\ln[(x-x')^2+y^2]$, and its difference (the remainder) from G_δ. This last value, remaining practically constant for all values of (x, y) near $(x',0)$ brings to light the dominant behavior of the singular term and the importance of extracting it out of G in closed form. In all cases the clear superiority of the expansions G_γ, G_δ over G_α, G_β is obvious, particularly, when the field point is close to the interface ($y \cong 0$). Only for large y do the four expansions become equivalent from the standpoint of the rate of convergence.

In Table II the source point is placed near the wall $x=a$, $x'=29.9$, while (x, y) moves near and around it. Now as dominant for G_β, G_δ we consider the sum of terms $D=-\frac{1}{2}\ln[(x-x')^2+y^2]+\frac{1}{2}\ln[(x+x'-2a)^2+y^2]$ of the source and its nearby image. The clear superiority of G_β, G_δ over G_α, G_γ, respectively, is again obvious as well as the insignificant contribution of all terms beyond the two dominant ones in the value of G_β, G_δ. To show this we provide three values of G in each case, corresponding to the number of terms M kept in the main series summations over m, as explained previously, namely, $M=1$, 10, and 70. Even with $M=1$ (only the first term of the series) G_β, G_δ have settled to their final values within a three or four digit accuracy. These values are of course very near the dominant term. So, the remaining terms of the series affect only a small residual part of G_β, G_δ. It is interesting to notice that as M increases G_β and G_δ approach the "final" value from above and below, respectively, being always very close to it. On the contrary, G_α, G_γ start from very different values and very slowly tend to the correct value (from below and above, respectively), but it would require very large values of M indeed to get an acceptable approximation, certainly $M \gg 70$ for the example of Table II. This is a further demonstration of the importance of extracting out of G the dominant terms in closed form, particularly for regions near or around singular points or points of rapid change of the function.

Finally, we may state, that the best expression for G is G_δ. It is at least equivalent to the other three in all regions with x' away from 0 and a and y away from 0 and definitely better than the others when either $y \cong 0$ or $x' \cong 0$ or a. In particular, for microstrip problems in which the strip comes close to the walls $x=0$ or a it has been shown [4] that G_δ is definitely superior.

Appendix

We start with the determination of the roots of the transcendental equation (30). It is obvious that they do not coincide with the roots of the factor $\sinh(\mu\pi b_k/a)$ because these values reduce (30) to the impossible relation $\pm\epsilon_k=0$ $(k=1.2)$. This, also, justifies passing the side A_2A_3 of the contour Γ through the point $\mu''=na/b_1$ $(n=1,2,\cdots)$. Writing now

$$\mu\pi b_1/a=u \qquad \mu\pi b_2/a=-\beta u, \qquad \beta=-b_2/b_1>0 \tag{A1}$$

we turn to the roots of the other factor

$$D(u)=\epsilon_1\coth u+\epsilon_2\coth(\beta u)=0. \tag{A2}$$

With $u=u'+iu''$ and $\coth(u'+iu'')=(1+i\tanh u'\cdot\tan u'')/(\tanh u'+i\tan u'')$, this relation reduces to

$$\begin{aligned} D(u)=\epsilon_1&\frac{\tanh u'(1+\tan^2 u'')}{\tanh^2 u'+\tan^2 u''} \\ &+\epsilon_2\frac{\tanh(\beta u')[1+\tan^2(\beta u'')]}{\tanh^2(\beta u')+\tan^2(\beta u'')} \\ &+i\left[\epsilon_1\frac{\tan u''(\tanh^2 u'-1)}{\tanh^2 u'+\tan^2 u''}\right. \\ &\left.+\epsilon_2\frac{\tan^2(\beta u'')[\tanh^2(\beta u')-1]}{\tanh^2(\beta u')+\tan^2(\beta u'')}\right]. \end{aligned} \tag{A3}$$

Now $\tanh u'$ and $\tanh(\beta u')$ have the same sign, since $\beta>0$; also, they both vary between -1 and 1. Thus the real part of $D(u)$ is zero only for $u'=0$. Therefore, $u=iu''$ and either (A2) or (A3) reduces to

$$\epsilon_1\cot u''=-\epsilon_2\cot(\beta u''). \tag{A4}$$

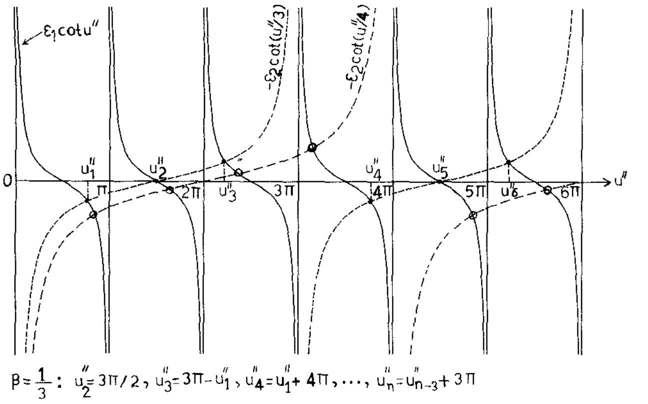

Fig. 3. The roots of the transcendental equation (A4) for $\beta = -b_2/b_1 = 1/3$ and $\beta = 1/4$.

Since $D(u)$ is odd we are only interested in the positive roots of (A4), which produce poles of $f_{kl}^{\{\mp\}}(\mu)$ inside Γ. Such roots are easy to determine numerically to any desired accuracy. In particular for $\beta = -b_2/b_1 = p$ or $1/p$, where p is an integer, only the first $p/2$ (p even) or $(p-1)/2$ (p odd) roots require numerical determination, the rest following by adding multiples of π. For instance, for $\beta = p = 1$, (A4) can be satisfied only for $\cot u'' = 0$, i.e., for $u'' = (2n-1)\pi/2$ $(n = 1, 2, \cdots)$ or $\mu'' = \mu_n = (2n-1)a/2b_1$. For $\beta = 1/3$, after determining numerically the root u_1'', there follows $u_2'' = 3\pi/2$, while $u_3'' = 3\pi - u_1''$. The rest of the roots follow by adding multiples of 3π to each of the first three, as illustrated in Fig. 3. On the same figure the case $\beta = 1/4$ is also illustrated; after determining numerically u_1', u_2'' there follows $u_3'' = 4\pi - u_2'', u_4'' = 4\pi - u_1''$ and the remaining roots are obtained by adding multiples of 4π to the first four. Similar simplifications for the solution of (A2) can be found in the more general case when β is the ratio of any two integers.

Finally, there remains to show that the integrand $f_{kl}^{\{\mp\}}(\mu)$ in (26) vanishes for all μ on A_1A_2 and A_2A_3 as these sides recede, independently, to ∞. Using the relation [11]

$$|\coth(u' + iu'')| = \left[\frac{\cosh 2u' + \cos 2u''}{\cosh 2u' - \cos 2u''}\right]^{1/2} \quad \text{(A5)}$$

we deduce that, for all values of u'', $|\coth u| \to 1$ as $u' \to \pm\infty$. Taking also into account that for $k = 1$ both $y \geq 0$ and $b_1 - y \geq 0$, while for $k = 2$ both $y \leq 0$ and $b_2 - y \leq 0$, it follows that as $\mu' = m + \frac{1}{2} \to +\infty$ (with μ on A_1A_2):

$$|f_{kl}^{\{\mp\}}(\mu)| \underset{\mu' \to +\infty}{\sim} \frac{\exp\left[\begin{Bmatrix} -|\mu''|\pi(1-x/a) \\ -|\mu''|\pi x/a \end{Bmatrix} - \mu'\frac{\pi}{a}|y|\right]}{\left[\left(\frac{\pi}{a}\right)^2(\mu'^2 + \mu''^2) + \left(\frac{q\pi}{b_l}\right)^2\right](\epsilon_1 + \epsilon_2)} \underset{\mu' \to +\infty}{\longrightarrow} 0. \quad \text{(A6)}$$

When $\mu'' = na/b_1 \to +\infty$ (with μ on A_2A_3) we first observe from (A1) that $u'' = n\pi$ and $\tan u'' = 0$. Therefore from (A3):

$$D(u) = \epsilon_1 \coth u' + \epsilon_2 \coth(\beta u')B - i\epsilon_2 F \quad \text{(A7)}$$

where B, F are positive quantities. Again $\coth u'$ and $\coth(\beta u')$ have the same sign, since $\beta > 0$, and $|\coth u'| \geq 1$, $|\coth(\beta u')| \geq 1$. It follows that

$$|D(u)| > \epsilon_1 + \epsilon_2 B \quad \text{and} \quad 1/|D(u)| < \frac{1}{\epsilon_1 + \epsilon_2 B} < \frac{1}{\epsilon_1}.$$

Therefore:

$$|f_{kl}^{\{\mp\}}| \underset{\mu'' \to +\infty}{<} \frac{\exp\left[\begin{Bmatrix} -\mu''\pi(1-x/a) \\ -\mu''\pi x/a \end{Bmatrix} - |\mu'|\frac{\pi}{a}|y|\right]}{\left[\left(\frac{\pi}{a}\right)^2(\mu'^2 + \mu''^2) + \left(\frac{q\pi}{b_l}\right)^2\right]\epsilon_1} \underset{\mu'' \to +\infty}{\longrightarrow} 0. \quad \text{(A8)}$$

References

[1] J. G. Fikioris, "On the convergence of orthogonal eigenfunction series," *Math. and Comput. in Simul.*, vol. 27, pp. 531–539, 1985.

[2] J. G. Fikioris and J. L. Tsalamengas, "Strongly and uniformly convergent Green's function expansions," *J. Franklin Inst.*, vol. 324, no. 1, pp. 1–17, 1987.

[3] J. G. Fikioris and J. L. Tsalamengas, "Exact solutions for rectangularly shielded lines by the Carleman–Vekua method," *IEEE Trans. Microwave Theory Tech.*, vol. 36, pp 659–675, Apr. 1988.

[4] J. G. Fikioris, J. L. Tsalamengas, and G. J. Fikioris, "Exact solutions for shielded printed microstrip lines by the Carleman–Vekua method," *IEEE Trans. Microwave Theory Tech.*, to be published.

[5] T. C. Edwards, *Foundations for Microstrip Circuit Design*. New York: Wiley, 1981.

[6] K. C. Gupta, R. Garg, and I. J. Bahl, *Microstrip Lines and Slotlines*. Dedham, MA: Artech House, 1979.

[7] N. G. Alexopoulos, "Integrated-circuit structures on anisotropic substrates," *IEEE Trans. Microwave Theory Tech.*, vol. MTT-33, pp. 847–881, Oct. 1985.

[8] D. L. Gish and O. Graham, "Characteristic impedance and phase velocity of a dielectric-supported air strip transmission line with side walls," *IEEE Trans. Microwave Theory Tech.*, vol. MTT-18, pp. 131–148, Mar. 1970.

[9] E. Yamashita and K. Atsuki, "Strip line with rectangular outer conductor and three dielectric layers," *IEEE Trans. Microwave Theory Tech.*, vol. MTT-18, pp. 238–244, May 1970.

[10] M. Kobayashi and R. Terakado, "General form of Green's function for multilayer microstrip line with rectangular side walls," *IEEE Trans. Microwave Theory Tech.*, vol. MTT-24, pp. 626–628, Sept. 1976.

[11] M. Abramowitz and I. A. Stegun, *Handbook of Mathematical Functions*. New York: Dover, 1972.

[12] D. M. Pozar, "A useful decomposition for the Green's functions of cylinders and spheres," *Radio Sci.*, vol. 17, no. 5, pp. 1192–1198, Sept.–Oct. 1982.

[13] A. Q. Howard, Jr., and D. B. Seidel, "Singularity extraction in kernel functions in closed region problems," *Radio Sci.*, vol. 13, no. 3, pp. 425–429, May–June 1978.

✠

John G. Fikioris was born in Sparta, Greece, on April 9, 1931. He received the Diploma of E.E. and M.E. from the National Technical University of Athens, Greece, in 1955, the M.S.E.E. degree of Rensselaer

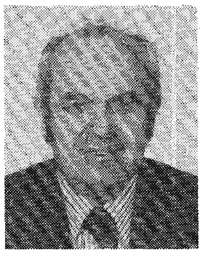

Polytechnic Institute, Troy, N.Y., in 1958, and the M.A. and Ph.D. degrees in applied physics from Harvard University, Cambridge, MA, in 1963.

From 1962 until early 1966, he worked as a Research Scientist with the RAD division of Avco Corporation, Wilmington, MA. From January 1966 to June 1972, he was Professor of Electrical Engineering at the University of Toledo, OH. In May 1972, he was elected Professor of Wireless and Long Distance Communications at the National Technical University of Athens, a position that he holds to date. His research contributions include topics in guiding phenomena, wave optics, antennas and wave propagation, diffraction and scattering, fundamental electromagnetic theory, and special mathematical techniques in applied electromagnetics.

Dr. Fikioris is a member of Sigma Xi.

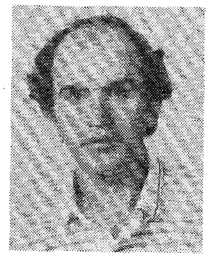

John L. Tsalamengas (M'87) was born in Karditsa, Greece, on April 26, 1953. He received the Diploma of Electrical and Mechanical Engineering and the doctor's degree in electrical engineering from the National Technical University of Athens (N.T.U.A.), Greece, in 1977 and 1983, respectively.

In 1983 he joined the Hellenic Aerospace Academy and worked there until the end of 1984. He then joined the Department of Electrical Engineering of N.T.U.A., first as a Research Associate and, in July 1987, as Assistant Professor of Electrical Engineering. His fields of interest include waveguide propagation, printed microwave (microstrip) devices, and boundary value problems in electromagnetic theory.

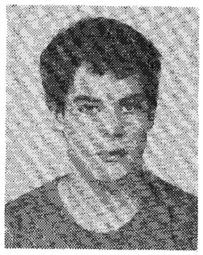

George J. Fikioris was born in Boston, MA, on December 3, 1962. He received the Diploma of Electrical Engineering from the National Technical University of Athens, Greece, in 1986. Since September of that same year he has been doing graduate work at the Division of Applied Sciences, Harvard University, Cambridge, MA. His main fields of interest are electromagnetics and applied mathematics.